E-proceedings of the 38th IAHR World Congress
September 1-6, 2019, Panama City, Panama
doi:10.3850/38WC092019-0279

TURBULENT MIXING AND TURBULENT EVENTS IN BREAKING BORES

RUI SHI[1], XINQIAN LENG[2] & HUBERT CHANSON[3]

[1,2,3] The University of Queensland, School of Civil Engneering, Brisbane QLD 4072, Australia
e-mail h.chanson@uq.edu.au

ABSTRACT

A breaking tidal bore is a highly turbulent transient process that may affect the natural estuarine system. Like many natural process flows, the tidal bore flow motion is dominated by coherent structure activities and turbulent events, with significant impact in terms of sediment processes. Herein an unsteady turbulent event analysis was developed for highly-unsteady rapidly-varied breaking bore flows. New experimental data were collected in a large size facility under controlled flow conditions. The data analysis was based upon basic concepts, in which turbulent bursting events were defined in terms of the instantaneous relative turbulent flux, and applied to the rapidly-varied highly-unsteady bore motion. The instantaneous three-dimensional velocities were recorded using an Acoustic Doppler Velocimetry. Rapid longitudinal deceleration, transient recirculation and large velocity fluctuations were observed during the bore passage, especially more intensive next to the sidewall. A turbulent event analysis was performed in the transient flow. The threshold constant k =1 was obtained from a sensitivity analysis. The unsteady turbulent event results highlighted an intense bursting process during the flow deceleration, in terms of the relatively large event duration, event amplitude and relative magnitude compared with the early flood flow phase. The unsteady event amplitude and relative magnitude exhibited a quasi-symmetrical distribution about the zero amplitude. The majority of turbulent events lasted between 0.005 s to 0.06 s. Overall, the results showed that the turbulent event analysis provided valuable quantitative details into the turbulent bursts that are responsible for major mixing and sedimentary processes.

Keywords: Turbulent events, Unsteady transient breaking bores; Physical modelling; Turbulent mixing.

1 INTRODUCTION

Turbulence in Nature is not a truly random process. Many geophysical flows are the locus of intense vortical structure activities and turbulent events. By definition, a turbulent event is a series of turbulent fluctuations containing more energy than the average turbulent fluctuations within a studied data set. Turbulent events are often associated with eddies and bursting, and play a major role in terms of sediment processes including scour, transport and accretion, as well as in contaminant mixing and dispersion (Nakagawa and Nezu 1981, Nielsen 1992). Turbulent event analyses have been successfully applied to a number of geophysical applications assuming quasi-steady flow conditions (Narasimha et al. 2007, Trevethan and Chanson 2010). Their application to transient flow situations is rarer (Leng et al. 2018).

In an estuary, a compression wave may propagate upstream as the result of macro-tidal conditions (tidal bores) or offshore tsunami generation (Chanson 2011, Tolkova et al. 2015, Reungoat et al. 2018). The shape of the bore is closely linked to its Froude number defined in its more general form as (Chanson 2012):

$$Fr_1 = \frac{V_1 + U}{\sqrt{g \frac{A_1}{B_1}}} \quad [1]$$

with V_1 the initially-steady flow velocity positive downstream U the bore celerity positive upstream, g the gravity acceleration, A_1 the initial flow cross-section area and B_1 the initial free-surface width. When the Froude number is less than 1.3 to 1.5, the bore is undular and no breaking is observed, except possibly next to the river banks (Peregrine 1966, Chanson 2010). For Fr_1 > 1.4 to 1.6, the leading edge of the bore presents a well-defined breaking roller (Hornumg et al. 1995) (Fig. 1). Figure 2 illustrates two breaking tidal bores.

In this study, a turbulent event analysis was developed for the highly-unsteady rapidly-varied surge flow following Leng et al. (2018) and applied to a breaking bore. The analysis was based upon the definition of turbulent bursting events in terms of the instantaneous relative turbulent flux. The method was applied to a detailed data set obtained in a large-size physical facility. The results provided insights into the complicated transient turbulent flow field beneath a breaking bore relevant to large-scale geophysical systems.

(a)

(b)

Figure 1. Breaking bore photographs. (a) breaking tidal bore of the Qiantang River (China) in early 1897 with bore propagation from left to right (Photograph by J. Cholnoky, courtesy of Dr Albert Koenig); (b) breaking tidal bore of the Sélune River (France) on 24 September 2010 with bore propagation from right to left (Photograph by H. Chanson)

2 PHYSICAL MODELLING

2.1 Experimental channel

The physical investigation was conducted at the University of Queensland in a 19 m long 0.7 m wide tilting flume, previously used by Leng (2018). The channel was made of glass sidewalls and smooth PVC bed. The water discharge was supplied by two pumps, with the maximum discharge of 0.101 m^3/s. The water was supplied through an upstream intake reservoir equipped with a series of baffles and flow straighteners, issuing the water to the flume through a smooth convergent intake. A fast closing Tainter gate was located at the downstream end of the channel at x = 18 m, where x is measured from the channel's upstream end (Fig. 1a). The Tainter gate was rapidly closed to generate the bore that propagated upstream. The duration of the gate closure was less than 0.3 s to minimise any impact of the gate on the bore characteristics. Figure 2 shows a photograph and sketch of the experimental apparatus.

2.2 Instrumentation

The water discharge was measured by a magneto flow meter with an accuracy of 10^{-5} m^3/s. The free surface elevation and fluctuation were measured non-intrusively using nine acoustic displacement meters (ADMs) Microsonic^{TM} Mic+25/IU/TC located along and above the flume (Fig. 2a). In the present study, the ADM sampling rate was 200 Hz.

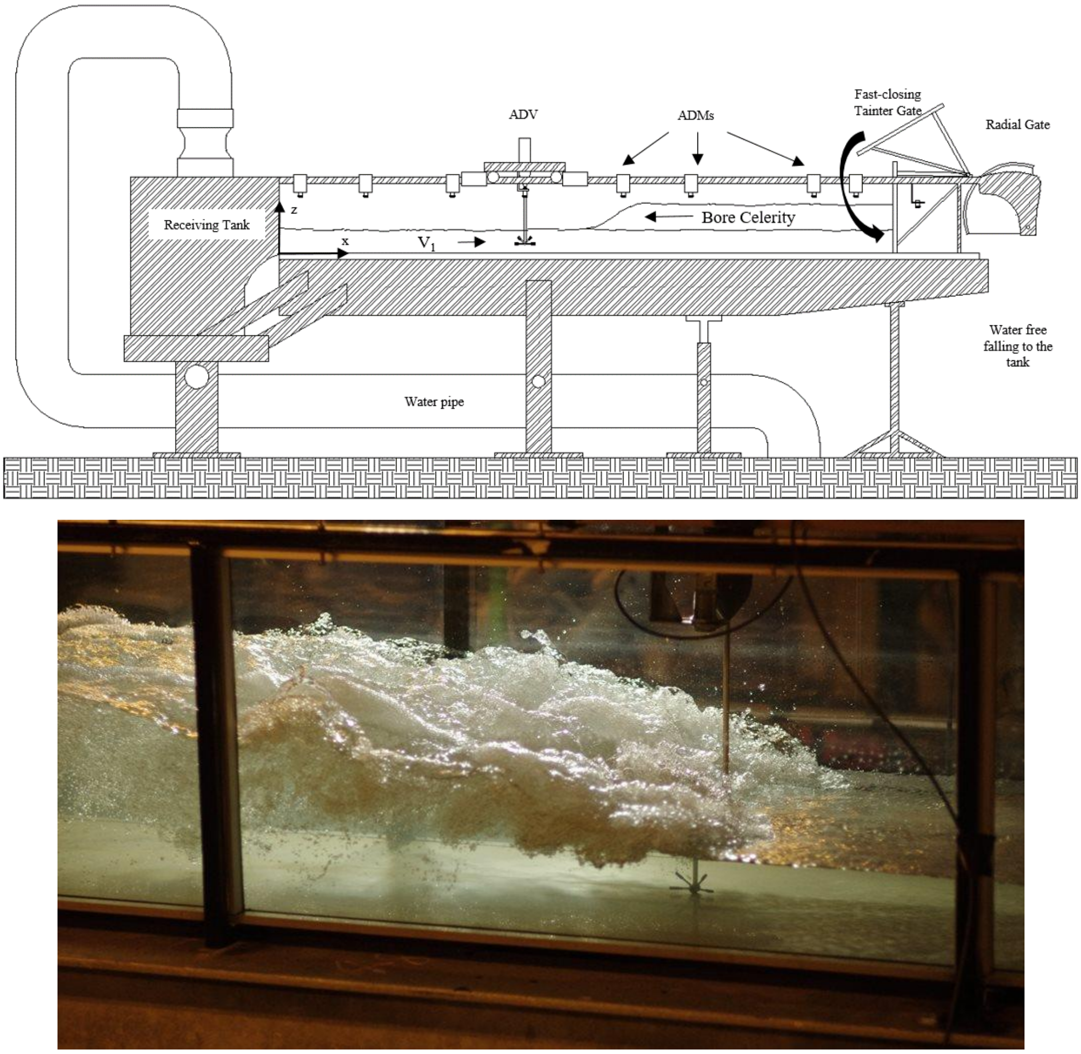

(a)

(b)

Figure 2. Experimental facility. (a) Distorted sketch of the experimental channel, with bore propagation from right to left. (b) Side view of a breaking bore propagation from left to right (Flow conditions: Q = 0.099 m^3/s, Fr_1 = 2.1, S_o = 0.0077); note the side-looking ADV head beneath the roller; shutter speed: 1/1,600 s.

An Acoustic Doppler Velocimetry (ADV) Nortek™ Vectrino+ (Serial No. VNO 0436) was used to record the instantaneous velocity in steady and unsteady flow conditions. The ADV had a three-dimensional side-looking head, as shown in Figure 2b. The ADV was installed at x = 8.5 m. The velocity range was set to be ± 2.5 m/s, with a sampling rate of 200 Hz, a transmit length of 0.3 mm and sampling volume of 1.5 mm. In steady flows, the ADV data filtering consisted of the removal of communication errors, average SNR less than 5 dB, and removal of average correlation less than 0.6. The data were further despiked using a phase-space thresholding technique. In the unsteady flow, the data filtering was limited to the removal of communication error.

2.3 Turbulent event analysis

A turbulent event was defined as a series of turbulent fluctuations that contain more energy than the average turbulent fluctuation. In the present study, the detection of the turbulence bursting events was based upon the technique of Narasimha et al. (2007). In quasi-steady flows, a turbulent event occurred when the absolute value of an instantaneous turbulent flux fluctuation, e.g. $q = v_x v_z$, was greater than the product of the standard deviation q' of the flux and a positive constant (Narasimha et al. 2007, Trevethan and Chanson 2010) (Fig. 3). Figure 3 shows a typical time variation of instantaneous flux fluctuations. In highly-unsteady transient flow, a standard deviation would be meaningless. Instead a turbulent event is defined by comparing the deviation of an instantaneous flux from its ensemble-median value with the difference between the third and first quartile times a threshold constant k:

$$\left|q-\bar{q}\right| > k\,(q_{75}-q_{25}) \qquad [2]$$

with $\bar{q}$ the ensemble-median flux, q_{75} the third quartile and q_{25} the first quartile. For a Gaussian distribution of the data, (q_{75}-q_{25}) would be equal to 1.3 times the standard deviation. The event duration τ, defined as the time integral between zero crossings in the flux fluctuation, may be linearly interpolated between a negative flux and a positive flux. The dimensionless amplitude A of a turbulent event is the ratio of the averaged flux for this event to the mean flux of the entire data set:

$$A = \frac{1}{\tau}\int_{\tau} \frac{q - \overline{q}}{\overline{q}} dt \qquad [3]$$

The relative contribution of an event to the total momentum flux of the data section is termed as the relative magnitude m defined as:

$$m = \frac{A\,\tau}{T} \qquad [4]$$

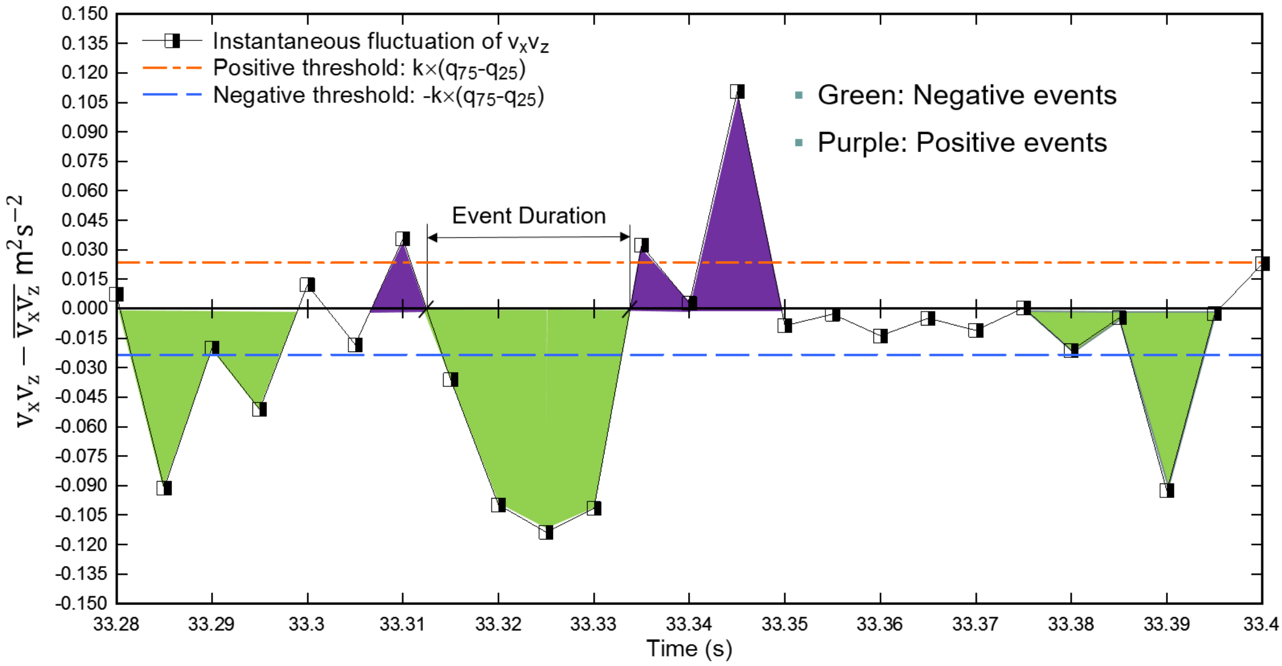

Figure 3. Turbulent flux event definitions in terms of the tangential stress v_xv_z for 33.28 s < t < 33.4 s. Record showing three positive events and three negative events - Flow conditions: Q = 0.099 m^3/s, S_o = 0.0077, x = 8.5 m, z/d_1 = 0.13, y/B = 0.5.

Past field works (Narasimha et al. 2007, Trevethan and Chanson 2010, Leng and Chanson 2018) used a threshold constant k = 0.77 (i.e. k=1/1.3). In steady flows, a sensitivity analysis was performed at a vertical location z/d_1 = 0.13 in terms of the turbulent fluxes v_xv_z and v_xv_y for 0 < k < 1.54. The results data showed a decreasing number of turbulent events with increasing the threshold constant k, with a large negative gradient for k < 0.77, which might be related to some electronic noise in the instrumentation. Both the median event duration, the dimensionless event amplitude and relative event magnitude increased with increasing threshold constant, regardless of the turbulent flux and the events. All the data showed larger gradients for k < 0.77, than for threshold constant k ≥ 0.77. The finding hinted that a high values of k would filter out a large amount of small-duration turbulent events. The effects of the threshold constant were also tested in terms of the first four statistic moments of the turbulent event duration, amplitude and magnitude at a vertical location (z/d_1 = 0.13). Fluctuating data were observed for k < 0.15, with monotonic data trends for k > 0.15. In summary, the sensitivity analysis in steady flow implied that any value within 0.77 ≤ k < 1.54 could be suitable. k = 0.77 was adopted herein.

In unsteady flows corresponding to a breaking bore, the transient flow motion consisted of two distinctive consecutive sequences: a rapid deceleration and an early flood flow immediately after the bore passage. A sensitivity analysis was similarly conducted in terms the threshold constant k in the deceleration and early flood flow sequence for 0 < k < 1.92. Figure 4 presents typical results for the deceleration phase (Fig. 4 Left) and early flood flow (Fig. 4 Right). With increasing threshold constant, the number of unsteady turbulent events per second decreased dramatically when k < 1, tending to some asymptote for k >1. The data showed a marked increase of unsteady turbulent event duration with increasing k for k < 1, with an almost constant trend for k > 1. The unsteady turbulent event amplitude and magnitude data showed symmetrical distributions of positive and negative events about x-axis, and an increase in absolute values with increasing k. The statistical properties of the event amplitude and magnitude were further analysed. Overall, a value k = 1 was adopted in unsteady bore flow.

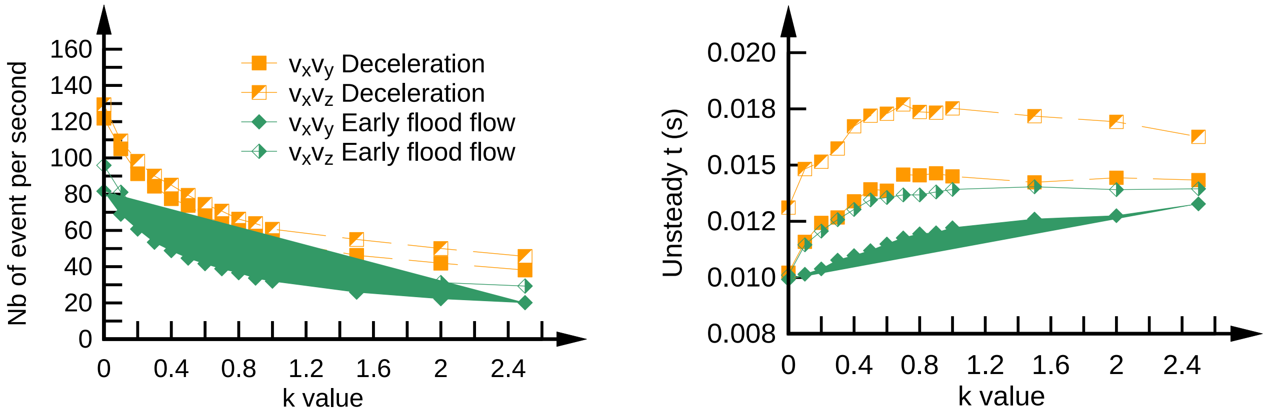

(A) Number of Unsteady turbulent event per second (B) Unsteady turbulent event duration

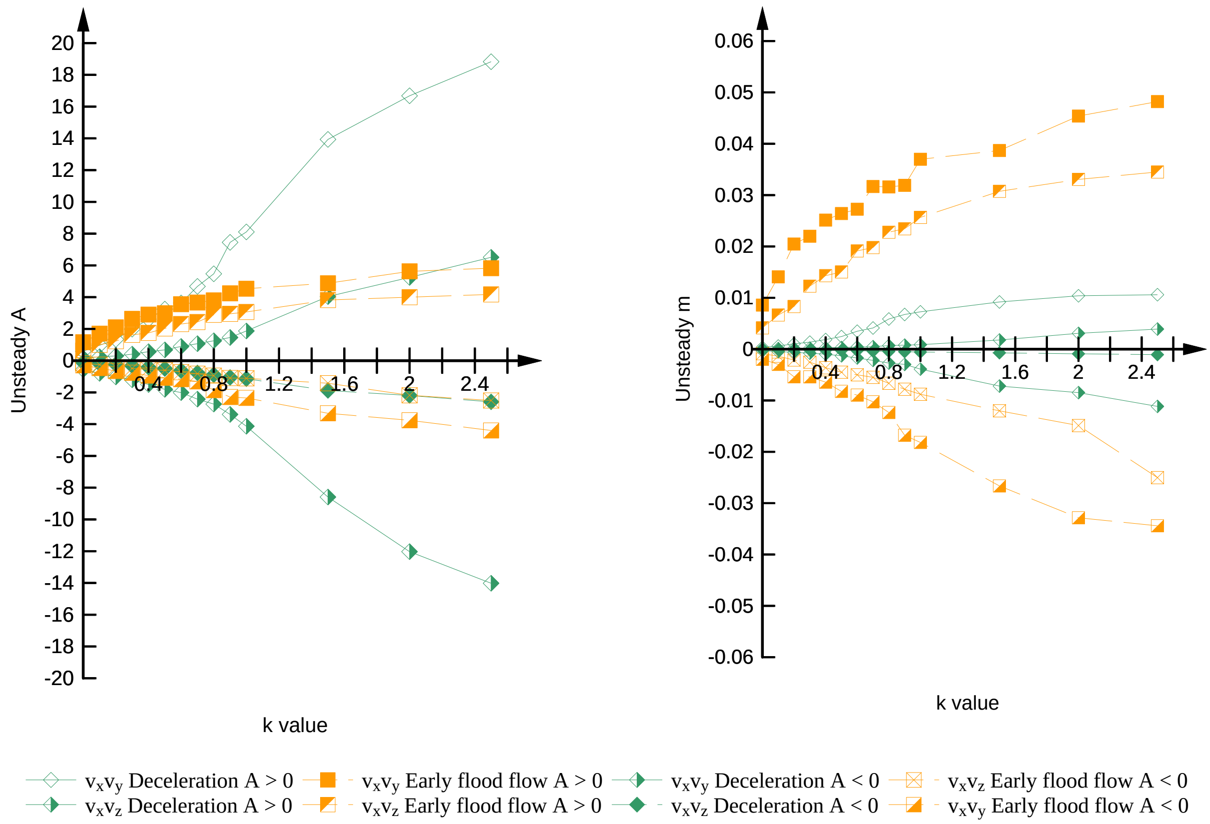

(C) Unsteady turbulent event amplitude (D) Unsteady turbulent event magnitude

Figure 4. Effect of the event threshold constant k on the ensemble-median turbulent event characteristics during the deceleration (Left) and early flood flow (Right) - Flow conditions: Q = 0.099 m^3/s, x = 8.5 m, z/d_1 = 0.067, y/B = 0.5, Fr_1 = 2.1.

2.4 Experimental programme

In the present study, a series of experiments were conducted systematically, with a focus on the free-surface measurement, unsteady velocity characteristics and turbulent event properties. The initial flow condition were a flow rate Q = 0.099 m^3/s, an initial depth d_1 = 0.09, with a bed slope S_o = 0.0077. A breaking bore was generated by closing rapidly and completely the Tainter gate. The bore propagated upstream with a celerity U = 0.6 m/s, corresponding to a bore Froude number Fr_1 = 2.1.

Both ADM and ADV units were sampled synchronously. All runs were synchronised using an ADM located immediately downstream of the gate, setting t = 0 at the date closure. To capture the unsteady nature of the turbulent flow, the experiments were designed to be highly repeatable, enabling an ensemble-averaged data analysis. The experiments were repeated 25 times and the results were ensemble-averaged.

3 FREE-SURFACE AND VELOCITY MEASUREMENTS

The propagation of breaking bores was a highly turbulent, three-dimensional process. The rapid gate closure induced a violent bore generation, with water piling up against the closed Tainter gate. The process was highly turbulent with intense aeration. Once formed, the bore initially accelerated, before decelerating until it reached a quasi-constant celerity U. At the sampling location (x = 8.5m), the bore was fully-breaking. The leading edge of the bore was a breaking roller, characterised by a sudden increase in flow depth, intensive air entrainment and strong turbulence mixing. The water surface ahead of the roller was flat and the passage of the roller induced a marked discontinuity in the water elevation (Fig. 2b).

With the passage of the bore, the ensemble-averaged longitudinal velocity data showed a marked deceleration for all the locations, and negative longitudinal velocities observed at in the end of deceleration process at the vertical locations near the channel bed (z/d_1 = 0.067 and 0.13), indicating transient recirculation next to the channel bed (Fig. 5a). This flow reversal motion was consistent with previous field works, experimental and numerical studies (Chanson and Toi 2015, Leng 2018). Both the transverse and vertical velocity data fluctuated about zero value in the steady flow, and they presented large fluctuations during and after the passage of the breaking roller (Fig. 5b). This finding hinted the occurrence of large vortical structure in the longitudinal or vertical directions. Next to the free-surface (z/d_1 = 0.91), the vertical velocity data showed a sharp and short increase during the passage of the breaking roller toe, linked to the streamline curvature (Leng and Chanson 2016).

The instantaneous velocity fluctuations V_{75-25} were defined as the difference between the third and first quartile: $V_{75-25} = (V_{75}-V_{25})$. All the data showed a sharp increase in velocity fluctuations during the bore passage, for all three velocity components, at all elevations and at all transverse locations. Figure 6 presents typical experimental data. The largest velocity fluctuations were observed at the lowest and highest sampling locations, z/d_1 = 0.067 and 0.91 respectively.

A comparison of velocity and velocity fluctuations performed at several transverse locations was conducted for y/B = 0.50, 0.70, 0.91 and 0.96, with y the transverse distance from the right sidewall. Overall, the data showed consistent trends in terms of the longitudinal velocity before and after the passage of breaking bores. Stronger transient recirculation was observed next the sidewall (y/d_1 = 0.91 and 0.96), marked by the pronounced negative longitudinal velocity at the end of deceleration process. The transverse velocity data showed a different trend next to the sidewall (y/d_1 = 0.91 and 0.96) (Fig. 5b). The velocity fluctuation data showed pronounced peaks during the passage of breaking bores at all transverse locations, although possibly larger next to the sidewall.

4 UNSTEADY TURBULENT EVENTS RESULTS

During the passage of the breaking bore, the rapid increase in water level induced a major change in both longitudinal and vertical velocity fields. Figure 7 presents unsteady turbulent event data in terms of the turbulent fluxes v_xv_z and v_xv_y on the channel centreline. The results showed consistent numbers of events per second between the two different flow phases. The duration of the v_xv_z events were larger than the duration of v_xv_y events. Figures 7c and 7d presented the median values of total event duration, positive event duration and negative event duration respectively. For a given turbulent flux v_iv_j, the duration of the deceleration phase were slightly larger than the event duration during the early flood flow, and the large number of events corresponded to small event durations. The data in terms of the unsteady event amplitude and relative magnitude for the positive event and negative events showed a quasi-symmetrical distribution about zero amplitude, indicating similar fluctuation behaviour between positive and negative events. For a given turbulent flux, the amplitude of the deceleration process was significantly larger than the amplitude of the early flood flow phase. For a given flow condition, the amplitude of v_xv_y were relatively higher than v_xv_z, implying a more intense turbulent process in the x-y plane. The relative magnitude data showed that the values during the deceleration phase were significantly higher than during the early flood flow motion, suggesting that the unsteady turbulent events had a major contribution to the total turbulent flux.

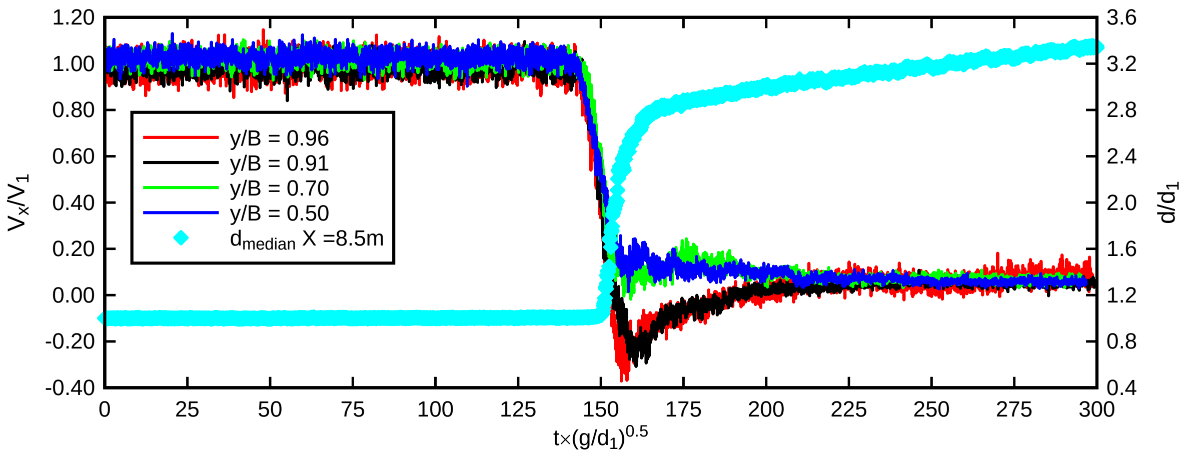

(A) Longtidual velocity V_x at the elevation z/d_1 = 0.13

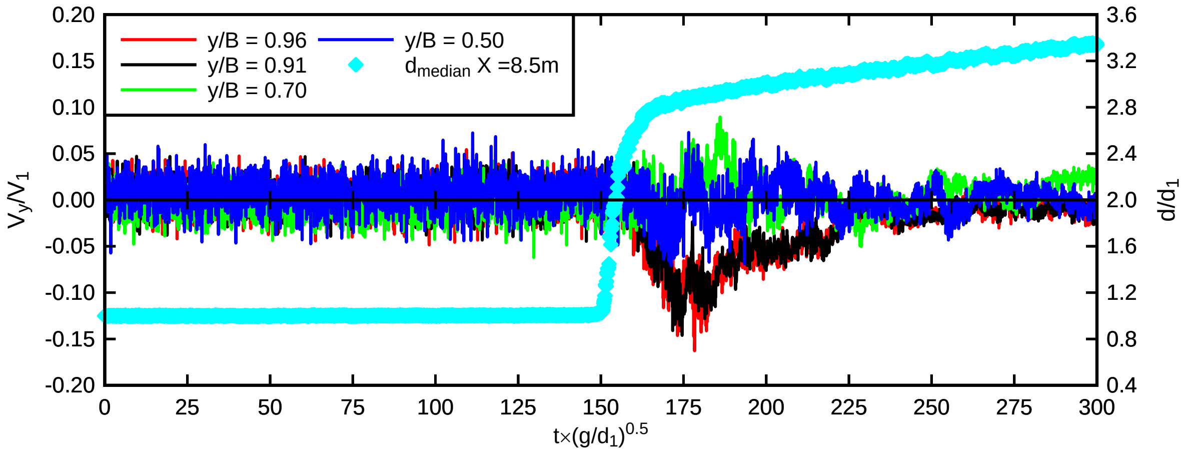

(B) Transverse velocity V_y at the elevation z/d_1 = 0.13

Figure 5. Dimensionless time variations of ensemble-averaged velocity in the longitudinal (A) and transverse (B) directions during the breaking bore passage at four transverse locations, with ensemble-averaged water depth measured at the velocity sampling location x = 8.5 m - Flow conditions: Q = 0.099 m^3/s, x = 8.5 m, z/d_1 = 0.013, y/B = 0.50, 0.70, 0.91, 0.96, Fr_1 = 2.1.

A comparison study of the unsteady turbulent event analysis at the vertical location y/d_1 = 0.13 was conducted for different transverse locations. The results showed transverse variations in turbulent event characteristics, without definite trend. The transverse fluctuations might reflect the three-dimensional nature of the bore roller, with the existence of transverse vortical structures discussed by Leng and Chanson (2015) and Chanson (2016).

Typical PDFs of instantaneous unsteady turbulent event duration and amplitude are presented in Figure 8 for the steady flow, deceleration phase and early flood flow. The data showed a right skewed distribution of the unsteady event duration, with majority of the data ranging from 0.005s to 0.06 s (Fig. 8a). The PDFs of event amplitude exhibit a quasi-symmetrical distribution in terms of zero value (Fig. 8b).

5 CONCLUSIONS

A physical study of breaking bore was undertaken in a large-size facility. The bore front was characterised by a discontinuity in water elevation, strong air entrainment and intense turbulence with large-scale three-dimensional coherent structures. The experiments were repeated systematically to derive the instantaneous ensemble-averaged flow properties. The free-surface and velocity measurements were performed using acoustic displacement meters (ADMs) and an Acoustic Doppler Velocimetry (ADV) at relatively high temporal resolution (200 Hz).The ensemble-averaged results showed an increase in the water depth and rapid decay in the longitudinal velocity during the bore passage. The comparison of velocity and velocity fluctuations at several transverse locations suggested stronger transient recirculation, more fluctuated transverse velocity and larger peak value of velocity fluctuations next to the sidewall.

A turbulent event analysis was developed for the transient flow. The sensitivity analysis of the threshold constant k suggested a value k = 1 in the unsteady bore flow. The unsteady turbulent event results showed that for a given turbulent flux $v_i v_j$, the deceleration phase experienced larger event duration, amplitude and relative magnitude than the early flood flow phase, indicating a more intense bursting process during the flow deceleration. The unsteady event amplitude and relative magnitude exhibited a quasi-symmetrical distributions about the horizontal axis. Larger value of the turbulent flux $v_x v_z$ implied a more intense turbulent process in the x-y plane. The majority of turbulent events had a duration between 0.005 to 0.06 s, with the absolute value of the event amplitude mainly less than 6. Overall, the results showed that the turbulent event analysis provided valuable quantitative details into the turbulent bursts that are responsible for major mixing and sedimentary processes.

ACKNOWLEDGEMENTS

The authors thank Jason Van Der Gevel and Stewart Matthews for technical assistance. The financial support of the School of Civil Engineering at the University of Queensland is acknowledged.

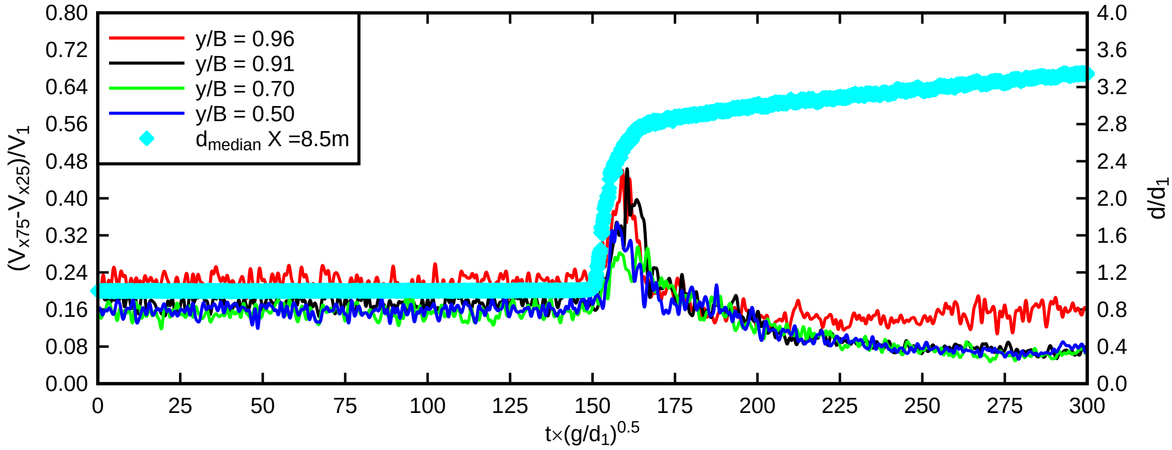

(A) Longitudinal velocity fluctuations V_{x75} - V_{x25} at the elevation z/d_1 = 0.13

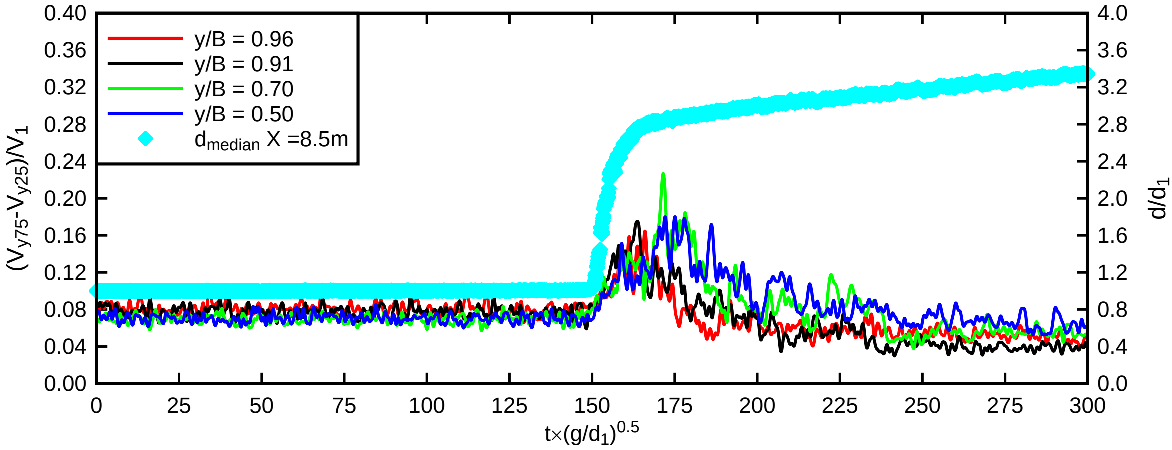

(B) Transverse velocity fluctuations V_{x75} - V_{x25} at the elevation z/d_1 = 0.13

Figure 6. Dimensionless ensemble-averaged time variations of longitudinal and transverse velocity fluctuations during the breaking bore passage at four transverse locations - Flow conditions: Q = 0.099 m^3/s, x = 8.5 m, z/d_1 = 0.013, y/B = 0.50, 0.70, 0.91, 0.96, Fr_1 = 2.1.

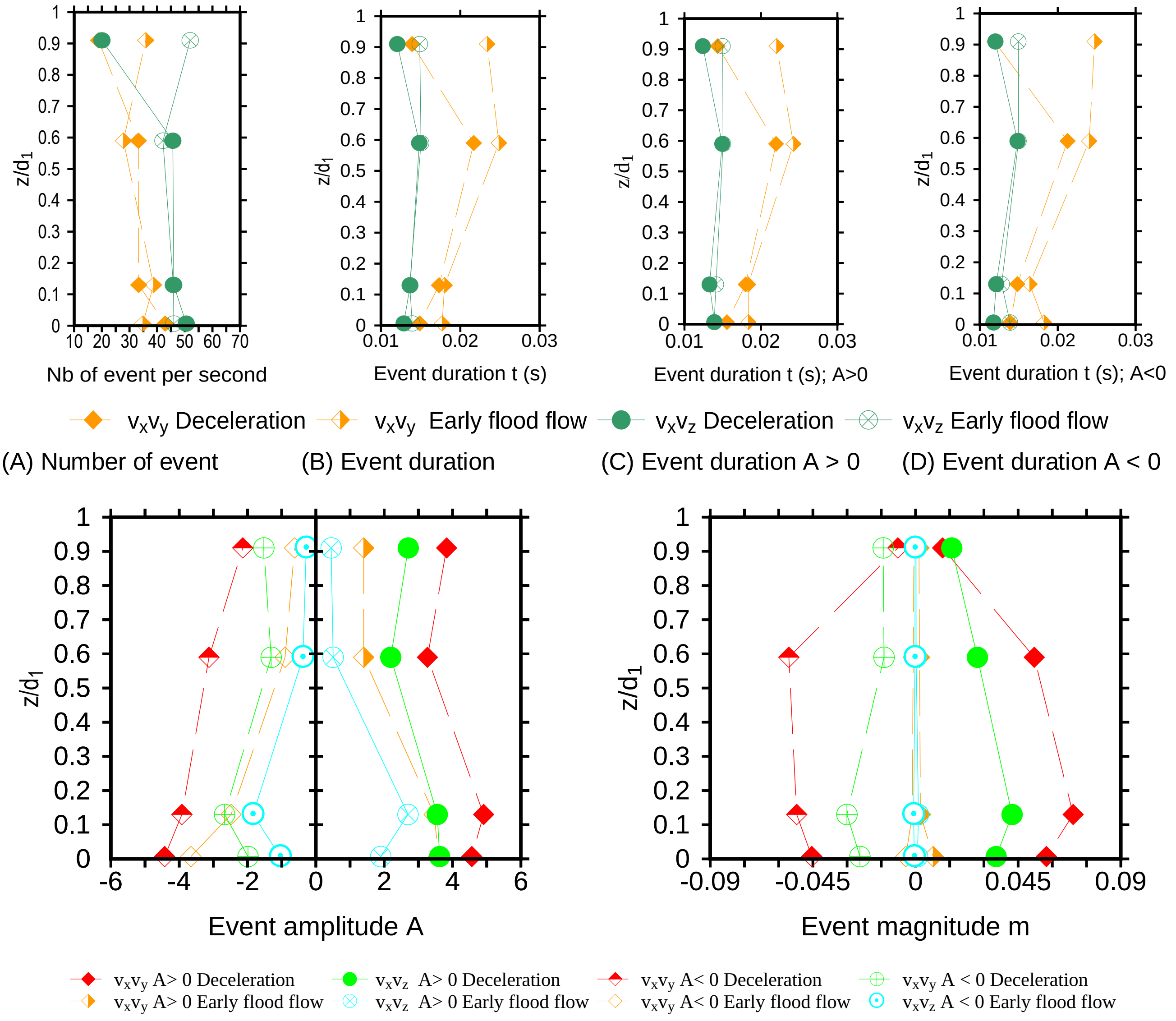

(A) Number of event (B) Event duration (C) Event duration A > 0 (D) Event duration A < 0

(E) Event amplitude (F) Event magnitude

Figure 7. Vertical distributions of ensemble-median values of unsteady turbulent event properties during deceleration and early flood flow phases on the channel centerline - Flow conditions: Q = 0.099 m^3/s, x = 8.5 m, Fr_1 = 2.1, y/B = 0.50.

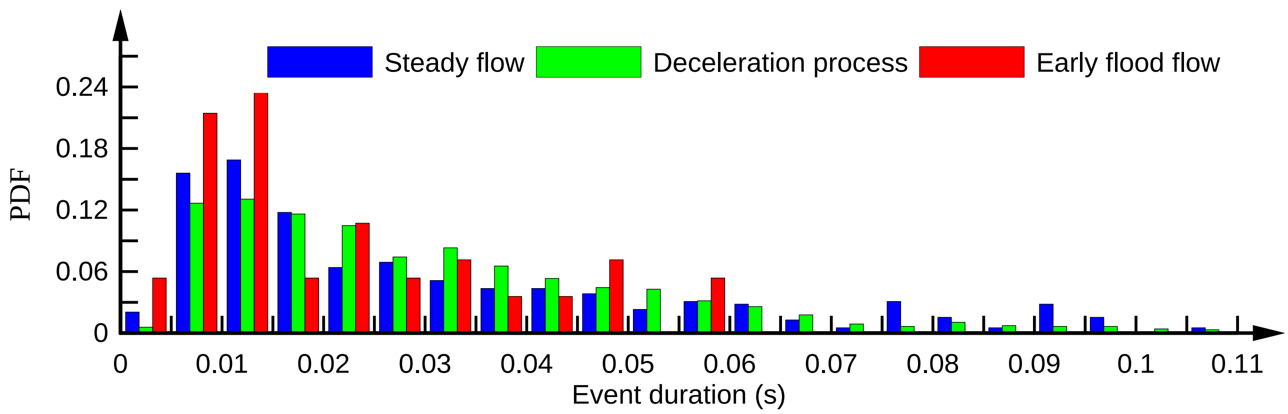

(A) PDF of event duration

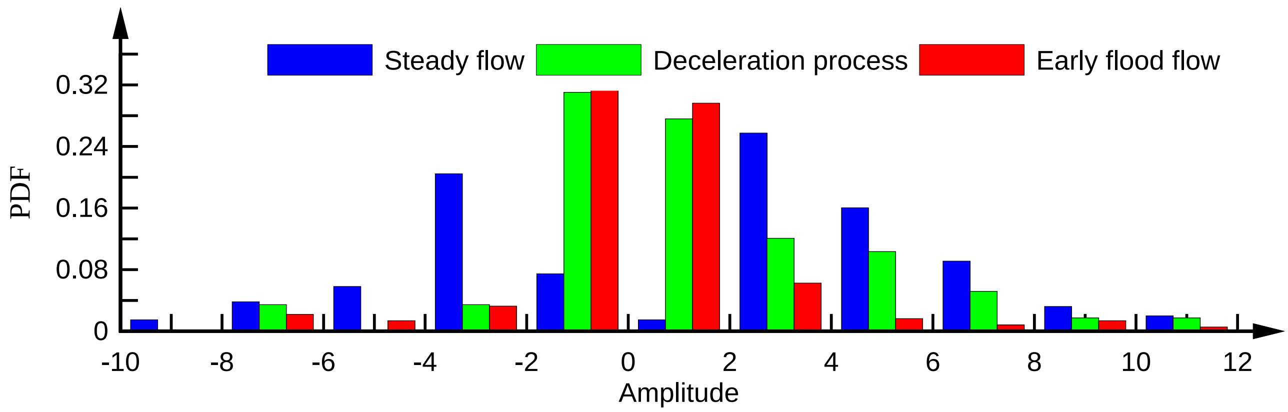

(B) PDF of amplitude

Figure 8. PDF of turbulent event duration and for turbulent flux v_xv_y - Flow conditions: Q = 0.099 m^3/s, x = 8.5 m, z/d_1 = 0.59, y/B = 0.50, Fr_1 = 2.1.

REFERENCES

Chanson, H. (2010). Undular Tidal Bores: Basic Theory and Free-surface Characteristics. *Journal of Hydraulic Engineering*, ASCE, Vol. 136, No. 11, pp. 940-944 (DOI: 10.1061/(ASCE)HY.1943-7900.0000264).

Chanson, H. (2011). *Tidal Bores, Aegir, Eagre, Mascaret, Pororoca: Theory and Observations*. World Scientific, Singapore, 220 pages (ISBN 9789814335416).

Chanson, H. (2012). Momentum Considerations in Hydraulic Jumps and Bores. *Journal of Irrigation and Drainage Engineering*, ASCE, Vol. 138, No. 4, pp. 382-385 (DOI 10.1061/(ASCE)IR.1943-4774.0000409).

Chanson, H. (2016). Atmospheric Noise of a Breaking Tidal Bore. *Journal of the Acoustical Society of America*, Vol. 139, No. 1, pp. 12-20 (DOI: 10.1121/1.4939113).

Chanson, H., and Toi, Y.H. (2015). Physical Modelling of Breaking Tidal Bores: Comparison with Prototype Data. *Journal of Hydraulic Research*, IAHR, Vol. 53, No. 2, pp. 264-273 (DOI: 10.1080/00221686.2014.989458).

Hornung, H.G., Willert, C., and Turner, S. (1995). The Flow Field Downstream of a Hydraulic Jump. *Journal of Fluid Mechanics*, Vol. 287, pp. 299-316.

Leng, X. (2018). Study of Turbulence: the Unsteady Propagation of Bores and Surges. *Ph.D. thesis*, School of Civil Engineering, The University of Queensland, Brisbane, Australia, 364 pages & 2 Digital Appendices (DOI: 10.14264/uql.2018.501).

Leng, X., and Chanson, H. (2015). Breaking Bore: Physical Observations of Roller Characteristics. *Mechanics Research Communications*, Vol. 65, pp. 24-29 (DOI: 10.1016/j.mechrescom.2015.02.008).

Leng, X., and Chanson, H. (2016). Coupling between Free-surface Fluctuations, Velocity Fluctuations and Turbulent Reynolds Stresses during the Upstream Propagation of Positive Surges, Bores and Compression Waves. *Environmental Fluid Mechanics*, Vol. 16, No. 4, pp. 695-719 & digital appendix (DOI: 10.1007/s10652-015-9438-8).

Leng, X., Chanson, H., and Reungoat, D. (2018). Turbulence and Turbulent Flux Events in Tidal Bores: Case Study of the Undular Tidal Bore of the Garonne River. *Environmental Fluid Mechanics*, Vol. 18, No. 4, pp. 807-828 (DOI: 10.1007/s10652-017-9561-9).

Nakagawa, H., and Nezu, I. (1981). Structure of Space-Time Correlations of Bursting Phenomena in an Open-Channel Flow. *Journal of Fluid Mechanics*, Vol. 104, pp. 1-43.

Narasimha, R., Kumar, S.R., Prabhu, A., and Kailas, S.V. (2007). Turbulent Flux Events in a Nearly Neutral Atmospheric Boundary Layer. *Phil. Trans. Royal Soc., Series A*, Vol. 365, pp. 841-858.

Nielsen, P. (1992). *Coastal Bottom Boundary Layers and Sediment Transport*. Advanced Series on Ocean Eng., Vol. 4, World Scientific Publ., Singapore.

Peregrine, D.H. (1966). Calculations of the Development of an Undular Bore. *Journal of Fluid Mechanics*, Vol 25, pp.321-330.

Reungoat, D., Lubin, P., Leng, X., and Chanson, H. (2018). Tidal Bore Hydrodynamics and Sediment Processes: 2010-2016 Field Observations in France. *Coastal Engineering Journal*, Vol. 60, No. 4, pp. 484-498 (DOI: 10.1080/21664250.2018.1529265).

Tolkova, E., Tanaka, H., and Roh, M. (2015). Tsunami observations in rivers from a perspective of tsunami interaction with tide and riverine flow. P*ure & Applied Geophysics*. Vol. 172, pp. 953-968 (DOI: 10.1007/s00024-014-1017-2).

Trevethan, M., and Chanson, H. (2010). Turbulence and Turbulent Flux Events in a Small Estuary. *Environmental Fluid Mechanics*, Vol. 10, No. 3, pp. 345-368 (DOI: 10.1007/s10652-009-9134-7).